

titcmt-94-4 (chao-dyn/9405003)

Numerical Study of Granular Turbulence and
the appearance of $k^{-5/3}$ energy spectrum without flow

Y-h. Taguchi

Department of Physics, Tokyo Institute of Technology
Oh-okayama, Meguro-ku, Tokyo 152 Japan

Abstract

The vibrated bed of powder, a vessel that mono disperse glass beads fill and a loud speaker shakes, is investigated numerically with the distinct element method, a kind of molecular dynamics. When the bed is heavily shaken, the displacement vectors of powder have the power spectrum with the dependence upon the wave number k as $k^{-5/3}$. The origin of this spectrum is suggested to be the balance between the injected and dissipative energy, analogous to the proposal by Kolmogorov to explain the $k^{-5/3}$ energy spectrum observed in the fluid turbulence. Furthermore, the same spectrum still appears even without flows of powder. Thus Kolmogorov's argument is more universal than believed before.

Keywords: granular turbulence, Kolmogorov scaling, numerical simulation, vibrated bed of powder.

1 Introduction

For these a few decades, the non-linear physics, which has remained untouched over several years since there is not any convenient method to investigate it, has become one of the central topics in the modern physics.

This is because the phenomenological approach provided by the statistical physics allows us to investigate them[1, 2]. The basic philosophy underlying this approach is: 'Some phenomena are independent of the details of the specific systems; Hence, the phenomenological approach will be valid.'

For example, the amplitude equation and the phase dynamics approach[1] can describe many phenomena ranging from the fluid dynamics to the chemical reaction. However, the validity of these approaches is restricted to the weak non-linear regime where only a few degrees of freedom survive.

On the other hand, the systems where many degrees of freedom still survive and couples with each other—the subjects of the most interest among non-linear physicists—are attacked by the phenomenological numerical approaches, like the coupled map lattice[2]. Although they exhibit many interesting phenomena, they lack the direct relations to the real systems. At the moment, there is not any general tool to study the real non-linear systems with many degrees of freedom surviving.

Instead of trying to find general tools, one can specify phenomena where many degrees of freedom survive, which appears in a real system with the easily treated model. It will become a start point to construct the general theory.

An example among the phenomena that have the surviving many degrees of freedom is the $k^{-5/3}$ energy spectrum in the fluid turbulence, which is first proposed by Kolmogorov[3]. In his theory, he has predicted that the energy spectrum of the fluid turbulence, in the high enough wave number regime, has the dependence upon the wave number k as $k^{-5/3}$, which was confirmed later experimentally and numerically. His theory is valid for almost all kinds of fluid turbulence:the experiments in the laboratories, the atmospheric flows—wind, and the flows in the tide. His success strongly supports the belief mentioned above:the details are not important. However, his theory is too general to make clear the mechanism from the dynamical points of view;it does not have any direct relationship to the Navier-Stokes equation:the basic equation of fluid motion.

The attempts to solidify the foundation of his theory have not yet succeeded, since it is hard to obtain enough informations of the local structures of the fluid turbulence. Experimentally, the simultaneous measurements of the velocity over the whole region is impossible. Only variables observed experimentally is the time sequence of the velocity at a specific point, which is interpreted as the spatial structure of the velocity by assuming unjustified Teylor's frozen turbulence hypothesis[3]. Numerically, although the detail of the velocity field is easily obtained, the limited computational resources makes the production of fully developed fluid turbulence

difficult.

Even phenomenological approaches are hardly applied to it. The amplitude equation or the phase dynamics approach cannot be applied to $k^{-5/3}$ energy spectrum where many degrees of freedom is essential. The phenomenological numerical approach has succeeded in reproducing them[4, 5], but could not explain the mechanism well due to the lack of the direct relationship to the experiment. Hence, for the fully understanding of the Kolmogorov's theory, it is hopeful to find the suitable substitution that obeys Kolmogorov's law and can be treated easily numerically and experimentally.

In this paper, the $k^{-5/3}$ energy spectrum is investigated in such a substitution:the granular flow. The granular systems, which many physicists are recently interested in[6, 7, 8, 9], are the systems whose number of degrees of freedom is limited enough to be integrated by the direct numerical simulations. For example, the number of degrees of freedom, even in the real experiments, is 10^6 , which should be compared with the Avogadro number 10^{23} that represents those of typical materials like fluids, liquids, and solids. The numerical simulations of the system with one hundred degrees of freedom reproduce the non-trivial properties originating in the strong non-linearity as seen in the next section. Therefore, we can expect the experimental correspondence between the numerical model and the real experiments.

The organization of this paper is as follows. In Sec.2, the results obtained numerically for the vibrated bed of powder is summarized. In Sec.3, to investigate the origin of the $k^{-5/3}$ law, the new model that has the experimental correspondence is introduced. Discussions and conclusions will be presented in Sec.4.

2 Numerical Granular Turbulence in Vibrated Bed of Powder

2.1 The experiment of vibrated bed of powder

The experimental setup of vibrated bed of powder is as follows[11, 12]. The flat vessel with the horizontal dimension of about 10 cm is filled with granular matter:typically, mono disperse glass beads having the diameter of about less than 1 mm. The bed is shaken vertically with the acceleration comparable to the gravity. The speaker is usually used for this purpose, the frequency of the vibration is about from 10 to 100 Hz, and the harmonic dependence upon time t is assumed;that is, the vertical displacement of the bed is as $b \cos \omega_0 t$. Although most experiments are performed in the three dimensional setups, the few did experiments in two dimensions.

When the acceleration amplitude, $\Gamma = b\omega_0^2$, exceeds some critical value Γ_c slightly larger than gravity acceleration g , the bed exhibits several non-trivial dynamical instabilities:the heaping, the convection[11, 12, 13, 14], the capillarity[15], the surface

fluidization[13, 16, 17], the Brazil nuts segregation[18, 19, 20, 21, 22], and the standing waves[23, 24, 25, 26], and so on.

2.2 Numerical Method—Distinct Element Method

The distinct element method (DEM), or the particle element method, was named analogous to the finite element method. Unlike in the finite element method, each element in DEM can move freely, but like in the finite element method represents the macroscopic property of the material. The individual granular particle is treated as an element obeying the visco-elastic equation,

$$\ddot{\mathbf{x}}_i = - \sum_{j=1}^N \theta(d - |\mathbf{x}_i - \mathbf{x}_j|) \left[k_0 \left\{ \mathbf{x}_i - \mathbf{x}_j - d \frac{\mathbf{x}_i - \mathbf{x}_j}{|\mathbf{x}_i - \mathbf{x}_j|} \right\} + \eta(\mathbf{v}_i - \mathbf{v}_j) \right] - \mathbf{g}, \quad (1)$$

where N is the total number of granular particles, \mathbf{x}_i is the position vector of the i th particle, \mathbf{g} is the gravity acceleration, and \mathbf{v} is velocity. Each particle has a diameter of d . Because of a step function $\theta(x)$, particles interact only when they contact with each other, which represents the discrete nature of the granular matter. k_0 and η are the elastic constant and the viscosity coefficient, respectively. This visco-elastic material constants give coefficient of restitution, e , and collision time t_{col} when two particles collide head-on; $e = \exp(-\eta\pi/\omega)$ and $t_{col} = \pi/\omega$ where $\omega = (2k_0 - \eta^2)^{1/2}$. In this sense, the visco-elasticity is not the real material property, but the phenomenological one. The DEM can be also considered as a simple molecular dynamics simulation having the above interactions.

Cundall and Struck[27], to investigate geological properties, has first proposed DEM which has come to have several versions later. However, in this paper, this simplified version, which can reproduce the convection[13, 14]—the most non-trivial phenomenon in the vibrated bed of powder, is used to study the vibrated bed of powder.

The above equations are integrated by the Euler scheme where the time increment Δt changes at each step so that the displacement during Δt of each particle does not exceeds some fixed value α (See appendix A).

To simulate the vibrated bed of powder, the granular particles move within the two dimensional space—to save the cpu time—with the bottom oscillating as a function of time t , $b \cos \omega_0 t$. In this representation the acceleration amplitude Γ , the strength of the external driven force, is $b\omega_0^2$. When the bottom collides with a granular particle, it reflects the particle with the elastic constant k_0 without the dissipation.

Figure 1: The process of fluidization. When $\Gamma < \Gamma_c$, the bed consists of the solid region. As Γ exceeds Γ_c , the fluid region appears, but the solid region still remains. For larger Γ , the bed is fully fluidized.

Figure 2: Numerical setups used in this section. The bed is horizontally periodic with the period of L_h , and the lid stays on the bed.

2.3 Numerical results in the vibrated bed of powder

First, the numerical behavior of the vibrated bed of powder obtained in the previous publications[13, 28, 29] is summarized. When Γ exceeds the gravity acceleration, the convection and the surface fluidization are observed[13]. The fluidized region where the flow exists has the finite depth which increases as Γ increases and coexists with the solid region where the powder does not flow (See Fig.1). To understand the dynamics of the vibrated bed of powder, we consider the granular flow in detail.

The granular flow is defined as the displacement of particle relative to each other. Thus, the motions like the translation and the expansion—not giving rise to the exchanges among particles—are not regarded as the flow in this subsection.

The numerical setup to measure the flow is shown in Fig.2, while the two dimensional space is horizontally periodic and has the oscillating bottom. On the granular layer lies the lid which never tilts and does obey the equation of motion

$$M \frac{d^2 h}{dt^2} = - \sum_{i=1}^N \theta(y_i - h) k_0 (h - y_i), \quad (2)$$

where M is the mass of the lid, h and y_i are the vertical coordinate (height) of the lid and the i th particle, respectively. Each particle collides with the lid elastically—with k_0 —and never pass through it. The lid suppresses the surface diffusion which causes the much larger displacement than the granular flow does.

The lid is also necessary to know when to record the positions of particles to calculate the granular flow. When vibrating, the bed expands and contracts repeatedly and thus does not keep the constant volume. To remove the contribution of these motions to the displacements, which are much larger than those of the granular flow, we define the measuring time t_n when the spacing $\Delta h(t)$ (See Fig.2) between the lid and the bottom has some definite value, h_0 . It enables us to measure the displacement under the condition of the constant volume and to exclude the contribution of the volume changes to the displacement of each particle. Thus the definition of the displacement vector is as

$$\Delta \mathbf{x}_i^{(n)} \equiv \mathbf{x}_i(t_{n+1}) - \mathbf{x}_i(t_n). \quad (3)$$

The typical displacement vectors in the fully fluidized bed with $\Gamma = 2.19$ ($\omega_0 = 2\pi/6, b = 2.0, N = 1024, L_h = 128, e = 0.8, t_{col} = 0.1, d = 2.0, g = 1.0, M =$

Figure 3: Typical displacement vectors of fully fluidized bed ($\Gamma = 2.19$)

Figure 4: The dependence of the power spectrum $S(K, Y)$ of the fully fluidized bed upon the wave number K and the height from the bottom Y ($\Gamma = 2.19$). (a) $Y = 1 \sim 5$, (b) $Y = 6 \sim 10$, (c) $Y = 11 \sim 15$, (d) $Y = 16 \sim 20$. The straight lines indicate the $K^{-5/3}$ dependence. For large Y , i.e. near the surface, the spectrum becomes flat in the high wave number region.

$100, h_0 = 34.0^1$) is shown in Fig.3. The spatial structure looks the velocity field in the turbulent fluid having the power spectrum with the $k^{-5/3}$ dependence upon the wave number k .

To compare it with the spatial structure of the velocity field in the fluid turbulence, Fourier power spectrum is calculated from the displacement vectors. First, I divide whole two dimensional space into d (horizontal) $\times \sqrt{3}d/2$ (vertical) cells. Each cell moves with the bottom and having numbers (X, Y) where X, Y are positive integers. The cell (X, Y) covers the area $d(X - 1/2) < x < d(X + 1/2), d(Y - 1/2) < y < d(Y + 1/2)$, where x and y are horizontal and vertical coordinates that have its origin on the bottom.

I define displacement vector on each cell as:

$$\Delta \mathbf{x}_{X,Y}^{(n)} \equiv \sum_{i \in (X,Y)} \Delta \mathbf{x}_i^{(n)}, \quad (4)$$

where summation runs over only particles in the cell (X, Y) . I calculate Fourier power spectrum for $\Delta \mathbf{x}_{X,Y}^{(n)}$ on each layer

$$S(K, Y) \equiv \langle \left| \sum_X \Delta x_{X,Y}^{(n)} \exp(-j2\pi XK/L) \right|^2 \rangle_n, \quad (5)$$

where K and L are integers, L is L_h/d . $\Delta x_{X,Y}^{(n)}$ is the horizontal component of $\Delta \mathbf{x}_{X,Y}^{(n)}$. j is a pure imaginary number. The average $\langle \dots \rangle_n$ runs over 30 periods.

Figure 4 shows the dependence of power spectrum upon the wave number K and the height from the bottom, Y . The power spectrum near the surface deviates from the straight line and has the flat spectrum—the white noise—in the higher wave number region, but for small Y , the power spectrum has the power dependence upon K . The slope of log-log plot is very close to $-5/3$ which coincides with that of the Kolmogorov's scaling theory. Therefore, we can conclude that the spatial structure in the vibrated bed is similar to that in the fluid turbulence.

¹For the dense packing the particle forms the triangular lattice which has the width of $L_h/d = 64$ and the height of $N/(L_h d) = 16$. Thus the height of the bed under the dense packing is $\frac{\sqrt{3}}{2} \times d \times \{(N/L_h d) - 1\} \sim 26.0$.

Figure 5: The dependence of the power spectrum $S(K, Y)$ of the almost solidized bed upon the wave number K and the height from the bottom Y ($\Gamma = 1.10$). (a) $Y = 1 \sim 5$. (b) $Y = 6 \sim 10$. (c) $Y = 11 \sim 15$. (d) $Y = 16 \sim 18$. For details, see Fig.4.

Figure 6: Typical displacement vectors of almost solidized bed. ($\Gamma = 1.10$)

The origin of this turbulent motion in the fluidized region should exist in the motion of solid region, because as shown in Fig.1 the solid region becomes fluidized gradually as Γ increases. To compare the motion in the solid region with that in the fluidized region, the power spectrum averaged over 64 periods in the solid region when $\Gamma = 1.10$ ($b = 1.0, h_0 = 30.0$, and the remaining parameters are identical to the above) is shown in Fig.5. As seen in the typical displacement vector (Fig.6), almost all region is solid—no exchange between particles, but the global structure of the power spectrum is qualitatively similar; the power spectrum in the lower layers has the power dependence upon K with the exponent $-5/3$, and the white noise appears in the higher wave number region for the upper granular layers.

In the following, I regard this $k^{-5/3}$ spectrum without flow as the origin of that seen in the fluidized region and make clear how the $k^{-5/3}$ spectrum appears without the flow.

3 The $k^{-5/3}$ power spectrum without flow

To understand the mechanism of the $k^{-5/3}$ power spectrum without flow, a model in which the powder does not flow is proposed. Each element, the granular particle, forms a triangular lattice² as shown in Fig.2 and interact, visco-elastically as described in Eq.(1) but without gravity \mathbf{g} , with the six neighbors. The bottom oscillates as before, but the lid does not obey the equation of motion, Eq.(2). Instead, the lid oscillate as a function of time, $b_0 \cos \omega_0 t$. That is, when the vertical coordinate of the bottom oscillate as $b \cos \omega_0 t$, then the height of the lid $h = h_0 + b_0 \cos \omega_0 t$. Thus, h_0 becomes the average distance between the bottom and the lid. At the initial stage, the granular particle lies on the triangular lattice between the bottom and the lid and moves obeying the Eq.(1) with $\mathbf{g} = 0$.

This numerical setup corresponds to the horizontally vibrated bed in the real experiments. One prepares the flat cell filled with the glass beads and makes two side walls oscillate harmonically. Hence, the following results are expected to be reproduced in the experiments.

²Hence no granular flow—no exchange between particles—is allowed at all

Figure 7: The time development of the energy spectrum, $E(K)$.(a) The initial state($t = 1.5$) and the early stage.(b) The medium stage where the high wave number components start to have flat part. (c)The late stage. The energy spectrum shows the system reach the thermal equilibrium state.

First, both the lid and the bottom oscillate with the same harmonic form, i.e. $b = b_0 = 1.0$, $\mathbf{g} = 0.0$. The h_0 is taken to be equivalent to the width of the triangular lattice having N/L rows, $\sqrt{3}/2 \times [(N/L)-1]$, and thus the granular particle is packed without space between each other. The remaining parameters are the same as used in the previous section.

Figure 7 shows the time development of the energy spectrum

$$E(K, t) \equiv \langle \left| \sum_{i=1}^L \Delta v_x(t; i, j) \exp(-j2\pi i K/L) \right|^2 \rangle_{j, \text{initial}}, \quad (6)$$

where $v_x(t; i, j)$ is the x component—the direction perpendicular to the direction of the vibration—of the velocity at the site (i, j) at time t . The average is taken over the layers— y direction—and the ten initial realization of the velocity with the white noise energy spectrum. One should notice that it is the true energy spectrum—not the power spectrum of the displacement vector as in the previous section—thus we can compare it with the Kolmogorov’s argument. At the initial time $t = 1.5$, each granular particle has the small random velocities and thus has the flat energy spectrum—the white noise. As time proceeds, the energy spectrum starts to incline and comes to have power dependence upon the wave number k . Furthermore, its slope is very close to the $-5/3$. However, for the medium stage, the flat spectrum appears in the higher wave number region and reaches the lower wave number region. Finally in the later stage, the total energy spectrum has become flat.

This process can be interpreted as follows. First, the energy starts to dissipate in the high wave number region where the energy dissipation rate takes the large value. It enables the system to reach the stationary state described by the Kolmogorov theory. However, the further injection of the energy dominates the dissipation and the system reaches the thermal equilibrium state:each mode has the same amount of the kinetic energy. This is also seen in the numerical simulation of the Navier-Stokes turbulence when the dissipation is not large enough. Therefore, the dynamics in the vibrated bed of powder is essentially equal to that of the fluid turbulence.

However, the $k^{-5/3}$ spectrum appears only temporally, contrast to the permanent appearance of it in the previous section. The dissipation in the vertically vibrated bed may be larger because the bed is compressed between the lid and the bottom. To take into account this effect, the value of b is taken to be 0 while b_0 remains unchanged so that the volume of the lattice changes. Starting from the initial white noise, the power spectrum becomes $k^{-5/3}$ one and returns to the flat one. However,

Figure 8: The dependence of the energy spectrum $E(K)$ upon the fraction of the cycle, $\omega_0 t = n\pi/6$. ($n = 1, 2, \dots, 6$). The $k^{-5/3}$ dependence is shown for the comparison.

Figure 9: the total energy, the energy input rate, and the energy dissipation rate as a function of time t (See appendix B).

this time the power spectrum recovers $k^{-5/3}$ dependence from the white noise and this process is repeated once a period of the oscillation(Fig.8). Here the energy spectrum is averaged over the ten periods to show the dependence upon the fraction of cycle. Thus $k^{-5/3}$ power spectrum can appear repeatedly if the effect of the compression is considered.

4 Discussion and Summary

In the previous section, the powder bed has the energy spectrum with $k^{-5/3}$. The results also suggest that the dissipation plays the important role. The behavior of the energy spectrum is coincident with that in the Navier-Stokes numerical simulation when the dissipation is not large enough. However, there is not the flow at all, thus one cannot expect the powder obeys the Navier-Stokes equation. So, what is the relation to the Kolmogorov theory proposed for the fluid flow?

Here the Kolmogorov's argument should be reconsidered. The essential assumption in the Kolmogorov's theory is that the balance between the energy input and the energy dissipation governs the dynamics of system. This means, the amount of total energy is as large as the product of the energy dissipation rate—or the energy input rate—and the characteristic time length. Figure 9 shows the total energy, the energy input rate, and the energy dissipation rate in the fluidized region investigated in Sec.2 as a function of time t . The total energy consists of both the elastic energy—among particles, the bottom, and the lid—and the kinetic and gravitational energy of particles and the lid. The dissipation energy comes from the viscosity between particles, and the work done by the vibrating bottom is considered as the energy input. The product between the energy input rate (\sim a few thousands) and the period of the vibration ($=6$) is about 10^4 . On the other hand, in Fig.9, the actual total energy is about 10^4 , when we eliminate the gravitational potential of the grand state($\sim 2 \times 10^4$). Thus, the total energy included in the bed is almost equal to the energy injected each period. This means, the balance between the energy input and the energy dissipation dominates the dynamics of the system. So far, the basic assumption necessary for the Kolmogorov's theory is satisfied.

The energy transport between the modes with the different wave number is also

Figure 10: The schematics of the energy flow in the vibrated bed.

assumed to be caused by the non-linearity, which the step function $\theta(x)$ in Eq.(1) has. Actually speaking, Kolmogorov has never used the existence of the flow to derive his scaling form, since it is apparent; the turbulence must flow. Here, the steady state which he proposed in his scaling theory can appear without the flow because the vibrated bed of powder can satisfy the basic requirements without the flow.

Another difference from the fluid is the dimensionality. The $k^{-5/3}$ spectrum can appear only in the three dimension, not in the two dimension where it appears in the powder. However, again, Kolgomorov has not used the dimensionality explicitly. The main difference between two and three dimension is whether there is another conserved variable, the enstrophy³. The enstrophy is impossible to define in the vibrated bed of powder because in the discrete material like the powder the spatial derivative, which is necessary to calculate the enstrophy, does not exist due to the lack of the continuity. Hence the enstrophy, which does not exist, cannot prevent the two dimensional system of the powder from obeying Kolmogorov's argument.

Assuming the $k^{-5/3}$ power spectrum comes from the Kolmogorov theory, we can explain the power spectrum seen in Sec. 2. For lower layers of the bed, the compression is strong enough, thus the clear $k^{-5/3}$ spectrum can be observed. However, the upper layers are not compressed enough to dissipate injected energy, which makes the energy stay in the high wave number region and causes the flat spectrum. Figure 10 shows the schematics of the energy flow in the vibrated bed considering the above discussions.

In summary, the vibrated bed of powder has the $k^{-5/3}$ power spectrum of the displacement vector. It comes from the local motions in the solid region which the Kolmogorov theory can explain. This means, I found that the steady state proposed by the Kolgomorov can appear even without flow; thus his theory is more universal than believed before. The real experiments should confirm these results.

This finding will make the effort to understand the $k^{-5/3}$ mechanism easier, since the powder system does not flow—thus we can use lattice representation, and the dimensionality is two—requiring smaller computational resources than the three dimension does. The efforts also may give rise to understand the general feature of the strongly non-linear system where many degrees of freedom survives and may give us the general method to study such systems.

³The enstrophy is defined as $\langle \omega(\mathbf{x}, t)^2 \rangle / 2$, where ω is the vorticity, $\text{rot} \mathbf{v}$.

5 Acknowledgement

This study is supported by Hosokawa-Powder Technology Foundation, Foundation for Promotion of Industrial Science, and Grant-in-Aid for Encouragement of Young Scientists (05740252) from the Ministry of Education, Science, and Culture, Japan.

A Numerical method to integrate the equation of motion

The method employed to integrate the equation of the motion Eq.(1) is Euler scheme,

$$\mathbf{x}_i(t + \Delta t) = \mathbf{x}_i(t) + \mathbf{v}_i(t)\Delta t + \frac{1}{2}\mathbf{a}_i(t)(\Delta t)^2 \quad (7)$$

$$\mathbf{v}_i(t + \Delta t) = \mathbf{v}_i(t) + \mathbf{a}_i(t)\Delta t, \quad (8)$$

where \mathbf{a}_i is the acceleration of i th particle. Eq.(7) enables us to relate the time increment Δt to $\Delta x_i(t) \equiv |x_i(t + \Delta t) - x_i(t)|$ and $\Delta y_i(t) \equiv |y_i(t + \Delta t) - y_i(t)|$, where x_i and y_i are the two components of \mathbf{x}_i respectively. Then

$$\Delta t_{xi} = \frac{\sqrt{v_{xi}^2 + 2a_{xi}\Delta x_i} - v_{xi}}{a_{xi}} \quad (9)$$

$$\Delta t_{yi} = \frac{\sqrt{v_{yi}^2 + 2a_{yi}\Delta y_i} - v_{yi}}{a_{yi}}, \quad (10)$$

$$(11)$$

where v_{xi} and v_{yi} are the x and y components of \mathbf{v}_i , and a_{xi} and a_{yi} are the x and y components of \mathbf{a}_i . Using these equations, the representation of Δt with $\Delta \mathbf{x}_i$, Δt takes the value of $\min_{\mathbf{x}_i} \Delta t_{\mathbf{x}_i}$ with the fixed Δx_i and Δy_i . In the present simulation, $\Delta x_i = \Delta y_i = \alpha = 0.005d$.

B The calculation of the energy and dissipation

In this appendix, the definition of several quantities appearing in Fig.9 is explained.

The total energy consists of the kinetic energy, the elastic energy, and the gravitational potential energy. The kinetic energy $E_{kinetic}$ is defined as,

$$E_{kinetic} = \frac{1}{2}M\mathbf{v}_{lid}^2 + \sum_{i=1}^N \frac{1}{2}\mathbf{v}_i^2, \quad (12)$$

where \mathbf{v}_{lid} is the velocity of the lid. The gravitational potential energy U_g can be expressed easily, too,

$$U_g = Mgh + \sum_{i=1}^N gy_i. \quad (13)$$

Here one should remember h is the height—the vertical coordinate—of the lid. The elastic energy U_{el} consists of those among the particles, the bottom plate, and the lid,

$$\begin{aligned} U_{el} &= \frac{1}{2}k_0 \left\{ \sum_{i,j} \theta(d - |\mathbf{x}_i - \mathbf{x}_j|)(d - |\mathbf{x}_i - \mathbf{x}_j|)^2 \right. \\ &\quad + \sum_{i=1}^N \theta(b \cos \omega_0 t - y_i)(b \cos \omega_0 t - y_i)^2 \\ &\quad \left. + \sum_{i=1}^N \theta(y_i - h)(y_i - h)^2 \right\}, \end{aligned} \quad (14)$$

Thus the total energy E_{tot} can be expressed as $E_{tot} = E_{kinetic} + U_g + U_{el}$.

The energy input rate E_{input} is the amount of work done by the bottom per unit time,

$$\begin{aligned} E_{input}^{(t)} &= \frac{1}{\Delta t} \sum_{i=1}^N [k_0 \{\theta(b \cos \omega_0 t - y_i(t))(b \cos \omega_0 t - y_i(t))\} \\ &\quad \times b \{\cos \omega_0(t + \Delta t) - \cos \omega_0 t\}]. \end{aligned} \quad (15)$$

Typically, Δt is taken to be 1×10^{-5} . The energy dissipation E_{dis} due to the viscosity between particles i and j is $\eta \int |(\mathbf{v}_i - \mathbf{v}_j) \cdot d(\mathbf{x}_i - \mathbf{x}_j)|$ when two particles contact with each other. Using $d(\mathbf{x}_i - \mathbf{x}_j)/dt = (\mathbf{v}_i - \mathbf{v}_j)$, we get $E_{dis} = \eta \int (\mathbf{v}_i - \mathbf{v}_j)^2 dt$. In the present discretization substituting $\mathbf{v}_i(t + \Delta t) = \mathbf{v}_i(t) + \mathbf{a}_i(t)\Delta t$,

$$E_{dis} = \frac{\eta}{\Delta t} \sum_{i,j} \theta(d - |\mathbf{x}_i - \mathbf{x}_j|) \left\{ \Delta \mathbf{v}_{ij}^2 \Delta t + \Delta \mathbf{v}_{ij} \cdot \mathbf{a}_{ij} (\Delta t)^2 + \frac{1}{3} \mathbf{a}_{ij}^2 (\Delta t)^3 \right\}, \quad (16)$$

where $\Delta \mathbf{v}_{ij} = \mathbf{v}_i - \mathbf{v}_j$ and $\Delta \mathbf{a}_{ij} = \mathbf{a}_i - \mathbf{a}_j$.

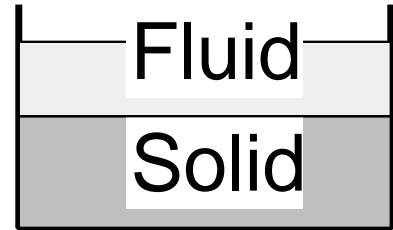
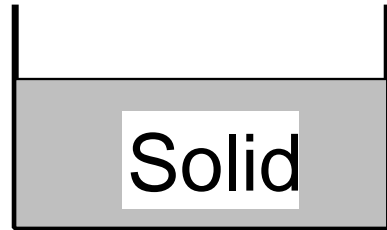
These above variables have the relation, $E_{tot}(t + \Delta t) = E_{tot}(t) + \{E_{input}(t) - E_{dis}(t)\}\Delta t + \mathcal{O}(\Delta t^2)$.

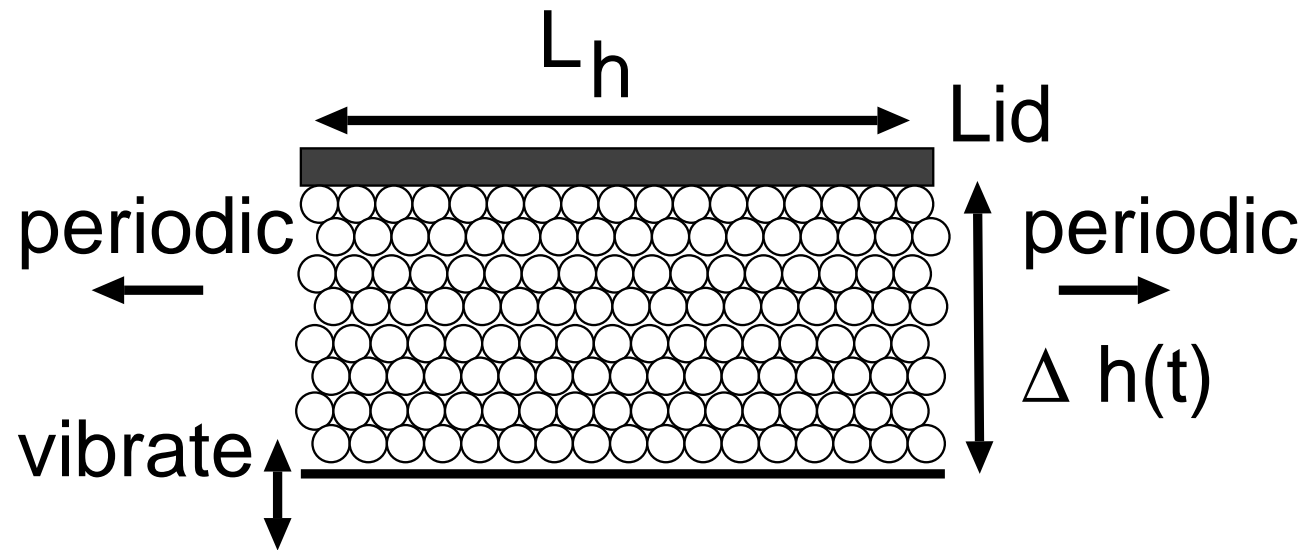
References

- [1] Y. Kuramoto, *Chemical Oscillations, Waves, and Turbulence*(Springer, Heidelberg, 1984)

- [2] K. Kaneko, *Collapse of Tori and Genesis of Chaos in Dissipative Systems* (World Scientific, Singapore, 1986)
- [3] A. Monin and A. Yaglom, Statistical Fluid Mechanics (MIT Press, Cambridge, 1971).
- [4] M. Yamada and K. Ohkitani, Phys. Rev. Lett. 60 (1988) 983.
- [5] Y-h. Taguchi and H. Takayasu, Physica D 69 (1993) 366.
- [6] H. M. Jaeger and S. R. Nagel, Science 255 (1992) 1523.
- [7] Y-h. Taguchi, H. Hayakawa, S. Sasa, and H. Nishimori eds., Dynamics of Powder Systems, Int. J. Mod. Phys. B 7 Nos. 9 & 10 (1993).
- [8] D. Bideau and A. Hansen eds., Disorder and Granular Media (North-Holland, Amsterdam, 1993).
- [9] A. Mehta ed., Granular Matter (Springer, Berlin, 1993).
- [10] C. Thornton ed., Powders and Grains '93 (A.A.Balkema Publishers, Rotterdam, 1993).
- [11] P. Evesque and J. Rajchenbach, Phys. Rev. Lett. 62 (1989) 44.
- [12] C. Laroche, S. Douady, and S. Fauve, J. Phys. (Paris) 50 (1989) 699.
- [13] Y-h. Taguchi, Phys. Rev. Lett. 69 (1992) 1367.
- [14] J. A. C. Gallas, H. J. Herrmann, and S. Sokołowski, Phys. Rev. Lett. 69 (1992) 1371.
- [15] T. Akiyama and T. Shimomura, Powder Technology 66 (1991) 243.
- [16] P. Evesque, E. Szmatala, and J-P. Denis, Europhys. Lett. 12 (1990) 623.
- [17] S. Luding, E. Clement, A. Blumen, J. Rajchenbach, and J. Duran, Phys. Rev. E 49 (1994) 1634.
- [18] A. Rosato, K. J. Strandburg, F. Prinz, and R. H. Swendsen, Phys. Rev. Lett. 58 (1987) 1038.
- [19] J. Duran, J. Rajchenbach, and E. Clément, Phys. Rev. Lett. 70 (1993) 2431.
- [20] R. Jullien, P. Meakin, and A. Pavlovitch, Phys. Rev. Lett. 69 (1992) 640.
- [21] T. Ohtsuki, Y. Takemoto, T. Hata, S. Kawai, and A. Hayashi, Int. J. Mod. Phys. B 7 (1993) 1865.

- [22] J. B. Knight, H. M. Jaeger, and S. R. Nagel, Phys. Rev. Lett. 70 (1993) 3728.
- [23] S. Douady, S. Fauve, and C. Laroche, Europhys. Lett. 8 (1989) 621.
- [24] H. K. Pak and R. P. Behringer, Phys. Rev. Lett. 71 (1993) 1832.
- [25] F. Melo, P. Umbanhower, and H. L. Swinney, Phys. Rev. Lett. 72 (1994) 162.
- [26] Dinkelacker F., Hübner A., and Lüscher E., Biol. Cybern. 56 (1987) 51.
- [27] P. A. Cundall and O. D. L. Strack, Geotechnique 29-1 (1979) 47.
- [28] Y-h. Taguchi, J. Phys. II (Paris) 2 (1992) 2103.
- [29] Y-h. Taguchi, Europhys. Lett. 24 (1993) 203.


$$\Gamma < \Gamma_c$$
$$\Gamma \gtrsim \Gamma_c$$
$$\Gamma \gg \Gamma_c$$



$$\Delta h(t)$$

